ISSN 1674-1056
http://cpb.iphy.ac.cn
http://iopscience.iop.org/cpb
中国物理 B
Chinese Physics
中国物理 Chinese Physics B

Coulomb exploded directional double ionization of N_2O molecules in multicycle femtosecond laser pulses

Junyang Ma(马俊杨), Kang Lin(林康), Qinying Ji(季琴颖), Wenbin Zhang(张文斌), Hanxiao Li(李韩笑), Fenghao Sun(孙烽豪), Junjie Qiang(强俊杰), Peifen Lu(陆培芬), Hui Li(李辉), Xiaochun Gong(宫晓春), Jian Wu(吴健)
Citation: Chin. Phys. B . 2019, 28(9): 093301 . **doi:** 10.1088/1674-1056/28/9/093301
Journal homepage: http://cpb.iphy.ac.cn; http://iopscience.iop.org/cpb

What follows is a list of articles you may be interested in

Effect of laser polarization on strong-field ionization and fragmentation of nitrous oxide molecules

Rui Wang(王瑞), Shi-Wen Zhang(张世文), Yang Liu(刘洋), Tian Sun(孙添), Hang Lv(吕航), Hai-Feng Xu(徐海峰)
Chin. Phys. B . 2019, 28(5): 053301 . **doi:** 10.1088/1674-1056/28/5/053301

Enhanced ionization of vibrational hot carbon disulfide molecules in strong femtosecond laser fields

Wan-Long Zuo(左万龙), Hang Lv(吕航), Hong-Jing Liang(梁红静), Shi-Min Shan(单石敏), Ri Ma(马日), Bing Yan(闫冰), Hai-Feng Xu(徐海峰)
Chin. Phys. B . 2018, 27(6): 063301 . **doi:** 10.1088/1674-1056/27/6/063301

Influence of the initial electronic state on minima of high-order harmonic spectrum radiated from hydrogen molecular ion

Hui-Fang Cui(崔会芳), Xiang-Yang Miao(苗向阳)
Chin. Phys. B . 2017, 26(10): 103302 . **doi:** 10.1088/1674-1056/26/10/103302

Ionizations and fragmentations of benzene, methylbenzene, and chlorobenzene in strong IR and UV laser fields

Zhang Jun-Feng, Lü Hang, Zuo Wan-Long, Xu Hai-Feng, Jin Ming-Xing, Ding Da-Jun
Chin. Phys. B . 2015, 24(11): 113301 . **doi:** 10.1088/1674-1056/24/11/113301

Theoretical approach to the study of vibrational effects on strong field ionization of molecules with alignment-dependent tunneling ionization rates

Zhang Mei-Xia, Yan Bing, Yang Yu-Jun, Luo Si-Zuo, Zhu Rui-Han, Yang Xue, Ding Da-Jun
Chin. Phys. B . 2015, 24(9): 093302 . **doi:** 10.1088/1674-1056/24/9/093302

SPECIAL TOPIC — Strong-field atomic and molecular physics

Coulomb exploded directional double ionization of N_2O molecules in multicycle femtosecond laser pulses*

Junyang Ma(马俊杨)[1], Kang Lin(林康)[1], Qinying Ji(季琴颖)[1], Wenbin Zhang(张文斌)[1], Hanxiao Li(李韩笑)[1], Fenghao Sun(孙烽豪)[1], Junjie Qiang(强俊杰)[1], Peifen Lu(陆培芬)[1], Hui Li(李辉)[1], Xiaochun Gong(宫晓春)[1], and Jian Wu(吴健)[1,2,†]

[1] State Key Laboratory of Precision Spectroscopy, East China Normal University, Shanghai 200062, China
[2] Collaborative Innovation Center of Extreme Optics, Shanxi University, Taiyuan 030006, China

(Received 27 May 2019; revised manuscript received 24 June 2019; published online 23 August 2019)

We experimentally investigate Coulomb exploded directional double ionization of N_2O molecules in elliptically polarized femtosecond laser pulses. The denitrogenation and deoxygenation channels are accessed via various pathways. It leads to distinct asymmetries in directional breaking of the doubly ionized N_2O molecules versus the instantaneous laser field vector, which is revealed by tracing the sum-momentum spectra of the ionic fragments as a recoil of the ejected electrons. Our results demonstrate that the accessibility of the Coulomb exploded double ionization channels of N_2O molecules are ruled by the detailed potential energy curves, and the directional emission of the fragments are governed by the joint effects of the electron localization-assisted enhanced ionization of the stretched molecules and the profiles of the molecular orbitals.

Keywords: strong-field ionization, directional molecular bond breaking, ultrafast dynamics of molecules

PACS: 33.80.Rv **DOI:** 10.1088/1674-1056/ab38aa

1. Introduction

Driven by a strong laser field, a molecule might break after removal of one or several electrons. The directional breaking of the molecular bond can be steered by using waveform controlled intense ultrashort laser pulses, which is significant for the manipulation of molecular chemical reactions. Governed by various mechanisms, it can be achieved by controlling the carrier envelope phase (CEP) of near-infrared few-cycle laser pulses[1–9] or the relative phase of two-color multicycle femtosecond laser pulses.[10–15] Recently, the directional bond breaking control was realized in two-dimensional space by using phase-controlled orthogonally or circularly polarized two-color laser fields.[16–18] However, the molecular bond breaking control mainly focused on the diatomic molecules, and only few triatomic[19–21] and polyatomic molecules[22–24] were investigated which are more interesting with rich dynamics.

In the present work, we experimentally investigate the Coulomb exploded double ionization of N_2O molecules, where two different channels are produced, i.e., $N_2O \rightarrow NO^+ + N^+ + 2e^-$ (labeled as denitrogenation channel) and $N_2O \rightarrow N_2^+ + O^+ + 2e^-$ (labeled as deoxygenation channel). As illustrated in Fig. 1(a), an elliptically polarized multi-cycle near-infrared femtosecond laser pulse is employed to drive the strong-field breaking of the molecules. Although this kind of optical symmetric laser pulse cannot control the directional breaking of the molecular bond, the bond breaking is intrinsically asymmetric and depends on the instantaneous vector of the oscillating laser field. We reveal such instantaneous asymmetry of the molecular bond breaking by gating on the ejection direction of the ionic fragments and tracing their sum-momentum spectra which encodes the instantaneous vector of the laser field at the ionization instants. Distinct asymmetries are observed and quantitatively analyzed for the denitrogenation and deoxygenation channels, allowing us to reveal various pathways.

2. Experimental setup

The measurements were performed in a standard reaction microscope of cold target recoil ion momentum spectroscopy (COLTRIMS),[25,26] as illustrated in Fig. 1(a). The molecular beam propagates along $+y$ and interacts with laser pulses (25 fs, 790 nm, 10 kHz) propagating along $+x$ after the focusing mirror ($f = 75$ mm) inside the ultrahigh vacuum apparatus. The polarization of the laser field is adjusted by using a half wave plate and a quarter wave plate in the laser beam. The intensities of the linearly polarized and elliptically polarized laser fields are the same in our experiments and estimated to be $I_0 \sim 6.0 \times 10^{14}$ W/cm^2. For the first ionization potential of N_2O (~ 12.9 eV),[27] the corresponding Keldysh parameter is calculated to be $\gamma \sim 0.43$ and thus we are mostly in the

*Project supported by the National Key R&D Program of China (Grant No. 2018YFA0306303), the National Natural Science Fundation of China (Grant Nos. 11425416, 11834004, and 11761141004), and the 111 Project of China (Grant No. B12024).

†Corresponding author. E-mail: jwu@phy.ecnu.edu.cn

© 2019 Chinese Physical Society and IOP Publishing Ltd

tunneling regime. As shown in Fig. 1(a), the elliptically polarized laser field rotates from $+z$ to $+y$ in the polarization plane, with major and minor axes of the laser field along y and z axes, respectively. The photoionization created ionic fragments were accelerated by the weak spectrometer field and to be detected in coincidence by a time and position sensitive microchannel plate detector at the end of the spectrometer. The three-dimensional momenta of the detected ions were reconstructed from the time-of-flights and the positions of the impacts. Atomic units (a.u.) are used throughout unless otherwise specified.

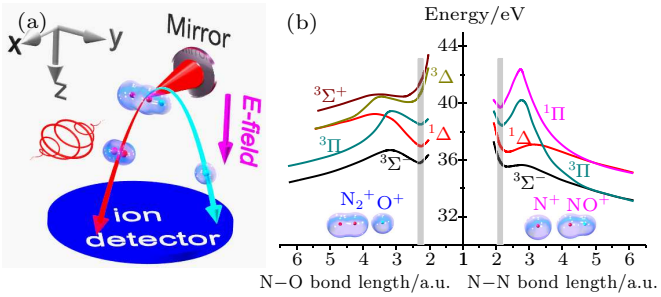


Fig. 1. (a) Scheme of the experimental apparatus. (b) Relevant potential energy curves of the N_2O^{2+}, adopted from Ref. [35]. The gray band indicates the Frack–Condon vertical transition range for the photoionization of N_2O.

3. Results and discussion

Figure 2(a) displays the momentum distributions of the denitrogenation and deoxygenation channels in y–z plane driven by a y-polarized laser field. The concentrated distribution along the laser polarization indicates that the molecular bond is more easily broken when the molecular axis is paralleled to the laser field. The angular distribution of the denitrogenation channel is relatively broader than the deoxygenation channel, in agreement with previous measurements performed using few-cycle near infrared laser pulses.[20] In the following, rather than control of the breaking of the molecular bond, we will focus on the intrinsic directional breaking of N_2O molecules as a function of the instantaneous vector of a near-infrared elliptically polarized ($\varepsilon \sim 0.86$) multi-cycle femtosecond laser pulse.

Driven by elliptically polarized laser fields, the electron recollision excitation is mostly suppressed and thus the double ionization of molecules mainly occurs via a sequential process by releasing two electrons one after the other. The sum-momentum of the two emitted electrons is the convolution of two individual electrons.[28,29] In our counter-clockwise rotating elliptically polarized laser field, the electrons are mainly released when the instantaneous laser field points to the $-y$ (or $+y$), which will end with a final momentum along $-z$ (or $+z$) as a consequence of angular streaking of the elliptically polarized pulse.[30] According to the law of momentum conservation of the breaking system, the correlated molecular ions receive an equivalent drift momentum in the opposite direction. Therefore, the electrons sum- momentum is mapped into the sum-momentum spectrum of the correlated fragment ions, e.g., $pz_{\rm sum} = pz_{\rm ion1} + pz_{\rm ion2} = -(pz_{\rm e1} + pz_{\rm e2})$ along the z axis, along which direction our apparatus has the best momentum resolution. The sum-momentum of the fragment ions reveal the instantaneous vector and strength of the rotating laser field at the instant of the electron release.

As mentioned above, the strong laser field ionization dynamics of N_2O depend on its bond orientation with respect to

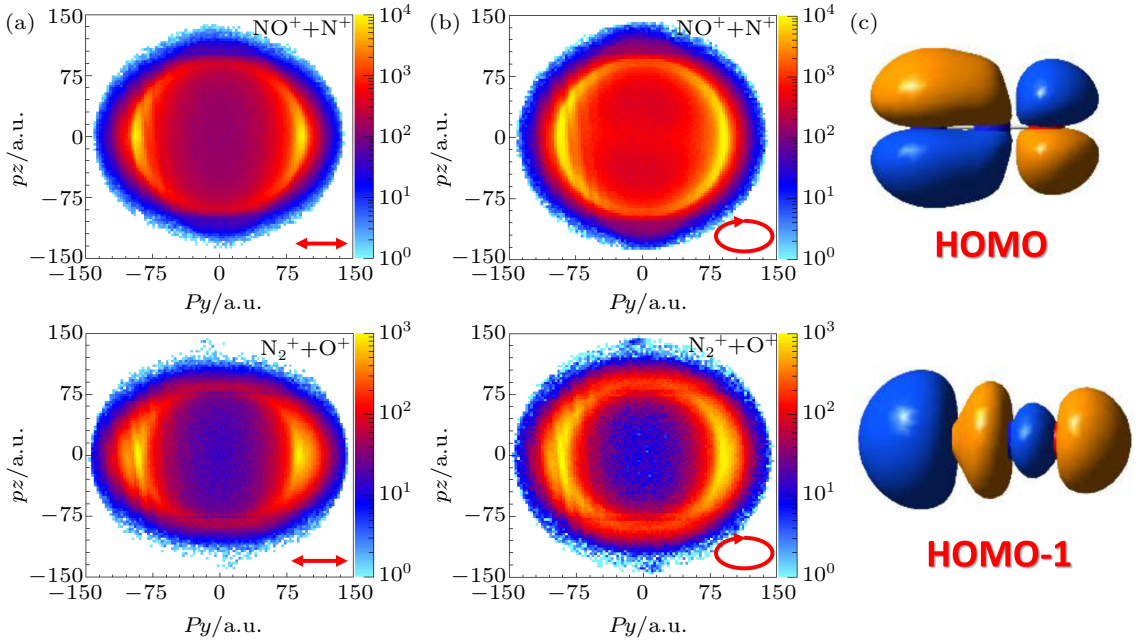


Fig. 2. Two-dimensional momentum distributions of the denitrogenation and deoxygenation channels driven by a linearly polarized (a) or elliptically polarized (b) laser field. The red arrow represents the polarization of the laser field. (c) The profiles of the HOMO and HOMO-1 of N_2O, where the nuclei N–N–O lie from the left to right sides.

the light polarization. The molecules aligned parallel to the major axis of the elliptically polarized laser field are predominantly ionized, as shown in Fig. 2(b). In the following discussion, we focus on the parallel orientated molecules by selecting fragment ions emitting within a conical angle of 30° with respect to the major polarization axis of the elliptically polarized laser field. The measured kinetic energy release (KER) dependent ion sum-momentum spectra along the z axis ($pz_{\rm sum}$) for the denitrogenation and deoxygenation channels are displayed in Figs. 3(a) and 3(d), respectively. Similar KER-dependent ion sum-momentum spectrum was observed for the denitrogenation channel in Ref. [21]. Rather than qualitatively, here we quantitatively analyze the asymmetries of the directional bond breaking of the doubly ionized N_2O molecules. Meanwhile, we distinguish the KER-dependent asymmetries, e.g., the high- and low-KER regions, of the fragmentation channels. This quantitative analysis allows us to identify different pathways towards various double ionization channels. The red solid curves and blue filled squares in Figs. 3(a) and 3(d) represent the ($pz_{\rm sum}$ integrated) KER spectrum and (KER integrated) $pz_{\rm sum}$ distributions, respectively. Here, the KERs of the fragments are carefully determined by calibrating the KER of the Coulomb exploded double ionization channel of the Ar dimers[31] measured in the same experimental setup. The three peak structure of the $pz_{\rm sum}$ spectrum corresponds to four possible sum-momenta of two sequentially released electrons.[29,32] The central peak results from the events where two electrons are ejected to opposite directions; while the two side peaks are filled by events where two electrons escape to the same side of the molecule. Asymmetric distributions of $pz_{\rm sum}$ are observed when we select the fragment ions N^+ or O^+ flying to $+y$ or $-y$, which are displayed in Figs. 3(b)–3(c) and 3(e)–3(f) (blue or red filled squares) for the denitrogenation and deoxygenation channels in different KER ranges, respectively. The asymmetric $pz_{\rm sum}$ spectra of two Coulomb exploded double ionization channels indicate that the N_2O molecules are preferred to be ionized when the laser field points from N to O, which agrees with previous observations using phase-controlled two-color femtosecond laser pulses or CEP controlled few-cycle laser pulses.[20,33]

To get quantitative insights of the asymmetric dissociative double ionization of N_2O molecules, we numerically fit the ion sum-momentum spectra by considering the convolution of the momenta of two sequentially released electrons,[29] as shown in Figs. 3(b) and 3(c) (denitrogenation channel), and in Figs. 3(e) and 3(f) (deoxygenation channel) (solid curves). For the denitrogenation channel, distinct asymmetries in $pz_{\rm sum}$ spectra are observed for the low KER (<6.3 eV) and high KER (>6.5 eV) regions. For the low-KER region, the numerical fits return $pz_{\rm e1}=0.82$ a.u, $pz_{\rm e2}=0.84$ a.u, $A_{1\pm}/A_{1\mp}=1.09$, and $A_{2\pm}/A_{2\mp}=1.37$. Here $pz_{\rm ek}$ are the magnitudes of the momenta of the released first ($k=1$) or second ($k=2$) electrons (corresponding to the strength of the laser field at the ionization instants), and $A_{k\pm}$ are the releasing probabilities of the first ($k=1$) or second ($k=2$) electrons when the laser field vector points from N to O (A_{k+}) or from O to N (A_{k-}) along the molecular axis, respectively. Thus, the ratio of $A_{k\pm}/A_{k\mp}$ stands for the asymmetry of the release of the first ($k=1$) or second ($k=2$) electrons by laser field vectors parallel or anti-parallel to the molecular bond. For the high-KER region, the numerical fit returns $pz_{\rm e1}=0.78$ a.u, $pz_{\rm e2}=0.93$ a.u, $A_{1\pm}/A_{1\mp}=1.05$, and $A_{2\pm}/A_{2\mp}=1.51$. However, for the deoxygenation channel, the asymmetry of the $pz_{\rm sum}$ spectra are very similar at different KER ranges. The numerical fits return $pz_{\rm e1}=0.76$ a.u, $pz_{\rm e2}=0.93$ a.u, $A_{1\pm}/A_{1\mp}=1.02$, and $A_{2\pm}/A_{2\mp}=1.97$ for the low-KER (<7.0 eV) region, and $pz_{\rm e1}=0.78$ a.u, $pz_{\rm e2}=0.95$ a.u, $A_{1\pm}/A_{1\mp}=1.02$, and $A_{2\pm}/A_{2\mp}=1.98$ for the high-KER (>7.5 eV) region. The different asymmetries of the $pz_{\rm sum}$ spectra correlated to the deoxygenation channel as compared to the denitrogenation channel suggests various pathways towards these two fragmentation channels.

The electronic configuration of the ground state of the N_2O molecule is $(1\sigma^2 2\sigma^2 3\sigma^2)(4\sigma^2 5\sigma^2)(6\sigma^2 1\pi^4 7\sigma^2 2\pi^4)$.[27] As shown in Fig. 2(c), the intramolecular electron density mainly concentrates around the N atoms for the HOMO and HOMO-1. The profile of the molecular orbital plays important roles in the laser field vector dependent ionization of molecules and thus the directional breaking of the molecular bond. Meanwhile, the binding energy of the electrons or the corresponding potential energy of the excited states governs the accessibility of various channels. As shown in Fig. 1(b), the potential curve of the lowest state correlated to the denitrogenation channel (right) is very shallow and thus more likely to dissociate as compared to that correlated to the deoxygenation channel (left). Therefore, the denitrogenation channel is preferred to be accessed by populating on the lower states than the deoxygenation channel which associates to higher excited states. It agrees with the fact that the yield of the denitrogenation channel is 5.6 times of the deoxygenation channel in our experiments.

As shown in Fig. 1(b), the three lowest electronic states ($^3\Sigma^-$,$^1\Delta$,$^1\Sigma^+$) of the N_2O dications are populated by removing two HOMO electrons, and the $^3\Pi$ and $^1\Pi$ states of the N_2O dications are occupied by individually removing two electrons from the HOMO and HOMO-1, respectively.[27,34,35] The photon ionization created nuclear wave packet (NWP) on the shallow $^3\Sigma^-$ and $^1\Delta$ states may directly dissociate to NO^+ and N^+ fragments, leading to the denitrogenation channel at high and low KERs, respectively. For instance, as illustrated in Fig. 1(b), for the denitrogenation channel with a dissociation limit of 28.8 eV, a KER of 7.1 eV is expected when it starts to dissociate from the equilibrium distance of the molecular bond ($R_{\rm N-N}=2.09$ a.u.) with a potential energy of 35.9 eV

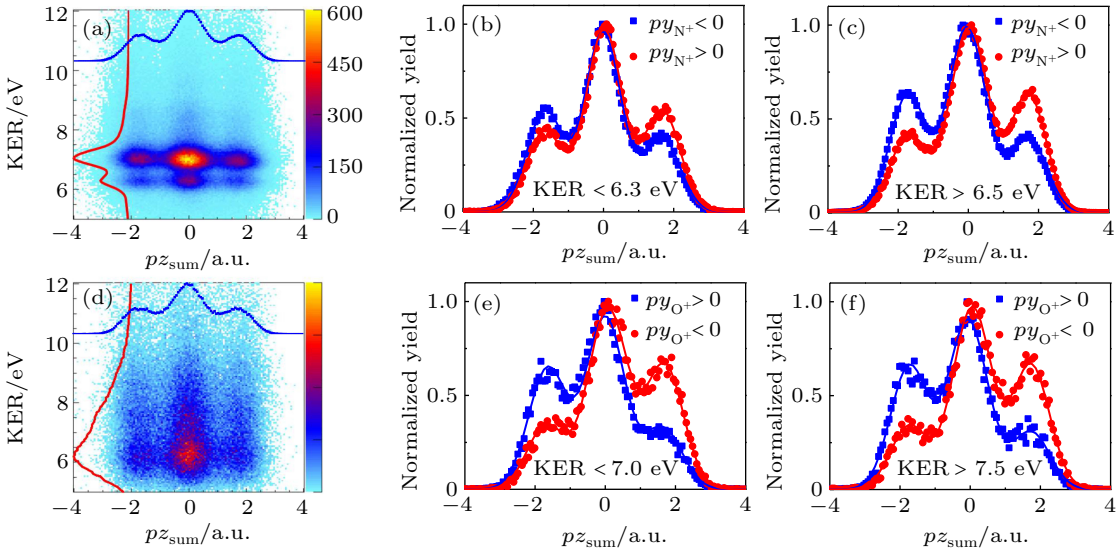


Fig. 3. The KER-dependent ion sum-momentum ($pz_{\rm sum}$) distributions of the denitrogenation (a) and deoxygenation (d) channels in elliptically polarized laser field, respectively. The red solid curves and blue filled squares in panels (a) and (d) represent the ($pz_{\rm sum}$ integrated) KER spectrum and (KER integrated) $pz_{\rm sum}$ distributions, respectively. The $pz_{\rm sum}$ distributions integrated over different KER ranges of the denitrogenation ((b), (c)) and deoxygenation ((e), (f)) channels (blue or red filled square) by gating the emission of the fragments N^+ and O^+ to $+y$ or $-y$ directions, respectively. The blue or red solid curves in panels (b), (c) and (e), (f) represent the fitting curves of the measured three peaks structure by using two Gaussians functions (see text).

on the $^3\Sigma^-$ state, which agrees well with the observed value of 7.0 eV in our experiments. The relatively lower yield of the low-KER region is because that the molecule needs to absorb one more photon from the laser field to populate the $^1\Delta$ state for the subsequent dissociation as compared to the high-KER region which directly dissociates along the $^3\Sigma^-$ state.

For the low-KER region of the denitrogenation channel, the drift momenta of the first and second electrons are almost equal which indicates that they are released by laser fields of similar intensities, i.e., either within a tiny time window or at different time with one in the rising edge and the other in the falling edge of the laser pulse. However, for the high-KER region, the drift momentum of the second electron is much larger than the first electron, which indicates that the second electron is released by a higher field strength.[28] Since the low-KER peak was absent in few-cycle laser pulses where the molecular bond does not have enough time to stretch,[20] we suggest that the first and second electrons are released in the rising and falling edges of the multi-cycle laser pulse separated by the bond stretching in producing the low-KER peak of the denitrogenation channel. Although the saturation effect in intense laser fields will also result in similar final momenta of the first and second electrons,[36] whose influence should be minor for the modest laser intensity used in our experiments. After the first ionization step, the molecular bond will stretch, which rearranges the distribution of the remaining electrons and alters their response to the light. For instance, the mechanism of electron localization-assisted enhanced ionization[37–41] will boost the ionization rate around the critical internuclear distance of the stretched molecule by releasing the electron from the up-field core at a relative low laser intensity. The denitrogenation channel is preferred to be produced when the laser field points from O to N owing to the mechanism of electron localization-assisted enhanced ionization, which is opposite to the expected asymmetry governed by the molecular orbital profile of HOMO in producing the low-KER region. As a result, the observed asymmetry of the low-KER region is smaller than the high-KER region. Many states of N_2O^+ are dissociative, for instance by populating the high vibrational levels of the $X^2\Pi$ state, the N–N bond of the N_2O^+ might stretch to a large separation for the enhanced ionization of the second electron. It may transit to the $^1\Delta$ state at around $R_{\rm N\text{-}N} = 3.2$ a.u. and afterwards dissociate with an expected KER of 6.2 eV, which agrees well with observed value of 6.2 eV in our experiments. Hence, in addition to the profile of the molecular orbital, the intramolecular rearrangement of the electron density distribution after the first ionization step, e.g., the electron-localization assisted enhanced ionization of stretched molecular ion, also plays an important role in the directional breaking of molecules. It depends on the detailed conditions of the experiments, such as the temporal duration and intensity of the laser pulses.[19]

Now let us discuss the pathways towards the deoxygenation channel. As shown in Figs. 3(b), 3(c), 3(e), and 3(f), the asymmetry of the $pz_{\rm sum}$ spectrum of the deoxygenation channel is larger than the denitrogenation channel. According to the numerical fits of the $pz_{\rm sum}$ spectra, the first electron released from HOMO is almost symmetric with respect to the laser field vector and molecular orientation; while the second electron released from HOMO-1 is more inclined to be released by laser field pointing from N to O. The pathway leading to the deoxygenation channel is as follows. By re-

moving one HOMO and one HOMO-1 electron, an NWP is created on the bound state of N_2O^{2+}, e.g., $^3\Pi$ state. It afterwards may be photon-coupled to the repulsive states (e.g., $^3\Delta$ or $^3\Sigma^+$ states) and dissociate into N_2^+ and O^+ fragments with different dissociation limits and thus a widespread KER spectrum. As shown in Fig. 2(a), the relatively broader angular distribution of the denitrogenation channel is observed as compared to the deoxygenation channel. Although the possible effects of dynamics orientation or angle-dependent post-dissociation may involve,[42] they actually cannot be excluded in our experiments, and their influence on the angular distributions are similar for various fragmentation channels. We hence attribute the observed different angular distributions of the denitrogenation and deoxygenation channels to the release of electrons from different molecular orbitals, e.g., the HOMO and HOMO-1 are four-lobed and bat-shape, respectively, as displayed in Fig. 2(c).

4. Conclusion

In summary, we have experimentally investigated Coulomb exploded directional double ionization of N_2O molecules in multi-cycle femtosecond laser pulses. By gating on the ejection direction of the fragment ions, asymmetric spectra of ion sum-momentum were observed for both the denitrogenation and deoxygenation channels, which indicates that the molecule prefers to be broken when the laser field points from N to O. Our results reveal the intrinsic asymmetry of the bond breaking versus the instantaneous vector of the laser field, which is determined by the joint effects of the profiles of molecular orbitals and the electron localization-assisted enhanced ionization of the stretched molecules in strong laser fields.

Acknowledgement

J. Ma acknowledges the support from the China Scholarship Council (CSC).

References

[1] Kling M F, Siedschlag Ch, Verhoef A J, Khan J I, Schultze M, Uphues Th, Ni Y, Uiberacker M, Drescher M, Krausz F and Vrakking M J J 2006 *Science* **312** 246
[2] Kremer M, Fischer B, Feuerstein B, de Jesus V L B, Sharma V, Hofrichter C, Rudenko A, Thumm U, Schröter C D, Moshammer R and Ullrich J 2009 *Phys. Rev. Lett.* **103** 213003
[3] Fischer B, Kremer M, Pfeifer T, Feuerstein B, Sharma V, Thumm U, Schröter C D, Moshammer R and Ullrich J 2010 *Phys. Rev. Lett.* **105** 223001
[4] McKenna J, Anis F, Sayler A M, Gaire B, Johnson N G, Parke E, Carnes K D, Esry B D and Ben-Itzhak I 2012 *Phys. Rev. A* **85** 023405
[5] Xu H, Xu T Y, He F, Kielpinski D, Sang R T and Litvinyuk I V 2014 *Phys. Rev. A* **89** 041403(R)
[6] Liu Y, Liu X, Deng Y, Wu C, Jiang H and Gong Q 2011 *Phys. Rev. Lett.* **106** 073004
[7] Betsch K J, Johnson N G, Bergues B, Kubel M, Herrwerth O, Senftleben A, Ben-Itzhak I, Paulus G G, Moshammer R, Ullrich J, Kling M F and Jones R R 2012 *Phys. Rev. A* **86** 063403
[8] Ursrey D and Esry B D 2017 *Phys. Rev. A* **96** 063409
[9] Znakovskaya I, von den Hoff P, Marcus G, Zherebtsov S, Bergues B, Gu X, Deng Y, Vrakking M J J, Kienberger R, Krausz F, de Vivie-Riedle R and Kling M F 2012 *Phys. Rev. Lett.* **108** 063002
[10] Ohmura H, Saito N and Tachiya M 2006 *Phys. Rev. Lett.* **96** 173001
[11] Ray D, He F, De S, Cao W, Mashiko H, Ranitovic P, Singh K P, Znakovskaya I, Thumm U, Paulus G G, Kling M F, Litvinyuk I V and Cocke C L 2009 *Phys. Rev. Lett.* **103** 223201
[12] Betsch K J, Pinkham D W and Jones R 2010 *Phys. Rev. Lett.* **105** 223002
[13] Wu J, Vredenborg A, Schmidt L Ph H, Jahnke T, Czasch A and Dörner R 2013 *Phys. Rev. A* **87** 023406
[14] Sheehy B, Walker B and DiMauro L F 1995 *Phys. Rev. Lett.* **74** 4799
[15] Charron E, Giusti-Suzor A and Mies F H 1993 *Phys. Rev. Lett.* **71** 692
[16] Gong X, He P, Song Q, Ji Q, Pan H, Ding J, He F, Zeng H and Wu J 2014 *Phys. Rev. Lett.* **113** 203001
[17] Lin K, Gong X, Song Q, Ji Q, Zhang W, Ma J, Lu P, Pan H, Ding J, Zeng H and Wu J 2016 *J. Phys. B: At. Mol. Opt. Phys.* **49** 025603
[18] Song Q, Lu P, Gong X, Ji Q, Lin K, Zhang W, Ma J, Zeng H and Wu J 2017 *Phys. Rev. A* **95** 013406
[19] Sakemi Y, Minemoto S and Sakai H 2017 *Phys. Rev. A* **96** 011401(R)
[20] Kübel M, Alnaser A S, Bergues B, Pischke T, Schmidt J, Deng Y, Jendrzejewski C, Ullrich J, Paulus G G, Azzeer A M, Kleineberg U, Moshammer R and Kling M F 2014 *New J. Phys.* **16** 065017
[21] Afaneh F and SchmidtB öcking H 2017 *Int. J. Mod. Phys. B* **31** 1750215
[22] Kübel M, Siemering R, Burger C, Kling N G, Li H, Alnaser A S, Bergues B, Zherebtsov S, Azzeer A M, Ben-Itzhak I, Moshammer R, de Vivie-Riedle R and Kling M F 2016 *Phys. Rev. Lett.* **116** 193001
[23] Li H, Kling N G, Gaumnitz T, Burger C, Siemering R, Schötz J, Liu Q, Ban L, Pertot Y, Wu J, Azzeer A M, de Vivie-Riedle R, Wörner H J and Kling M F 2017 *Opt. Express* **25** 14192
[24] Xie X, Doblhoff-Dier K, Roither S, Schöffler M S, Kartashov D, Xu H, Rathje T, Paulus G G, Baltuska A, Gräfe S and Kitzler M 2012 *Phys. Rev. Lett.* **109** 243001
[25] Dörner R, Mergel V, Jagutzki O, Spielberger L, Ullrich J, Moshammer R and Schmidt-Böcking H 2000 *Phys. Rep.* **330** 95
[26] Ullrich J, Moshammer R, Dorn A, Dörner R, Schmidt L Ph H and Schmidt-Böcking H 2003 *Rep. Prog. Phys.* **66** 1463
[27] Zhou X, Ranitovic P, Hogle C W, El, J H D, Kapteyn H C and Murnane M M 2012 *Nat. Phys.* **8** 232
[28] Wu J, Gong X, Kunitski M, Amankona-Diawuo F K, Schmidt L Ph H, Jahnke T, Czasch A, Seideman T and Dörner R 2013 *Phys. Rev. Lett.* **111** 083003
[29] Wu J, Schmidt L Ph H, Kunitski M, Meckel M, Voss S, Sann H, Kim H, Jahnke T, Czasch A and Dörner R 2012 *Phys. Rev. Lett.* **108** 183001
[30] Eckle P, Pfeiffer A N, Cirelli C, Staudte A, Dörner R, Muller H G, Büttiker M and Keller U 2008 *Science* **322** 1525
[31] Wu J, Vredenborg A, Ulrich B, Schmidt L Ph H, Meckel M, Voss S, Sann H, Kim H, Jahnke T, Czasch A and Dörner R 2011 *Phys. Rev. A* **83** 061403(R)
[32] Ma J, Li H, Lin K, Song Q, Ji Q, Zhang W, Li H X, Sun F, Qiang J, Lu P, Gong X, Zeng H and Wu J 2018 *Phys. Rev. A* **97** 063407
[33] Kotsina N, Kaziannis S, Danakas S and Kosmidis C 2013 *J. Chem. Phys.* **139** 104313
[34] Price S D, El, J H D, Fournier P G, Fournier J and Millie P 1988 *J. Chem. Phys.* **88** 1511
[35] Taylor S, El, J H D and Hochlaf M 2006 *J. Chem. Phys.* **124** 204319
[36] Wustelt P, Möller M, Rathje T, Sayler A M, Stöhlker T and Paulus G G 2015 *Phys. Rev. A* **91** 031401(R)
[37] Wu J, Meckel M, Schmidt L Ph H, Kunitski M, Voss S, Sann H, Kim H, Jahnke T, Czasch A and Dörner R 2012 *Nat. Commun.* **3** 1113
[38] Villeneuve D M, Yu M and Corkum P B 1996 *Phys. Rev. A* **54** 736
[39] Kamta G L and Bandrauk A D 2005 *Phys. Rev. Lett.* **94** 203003
[40] Lötstedt E, Kato T and Yamanouchi K 2012 *Phys. Rev. A* **85** 041402(R)
[41] Bocharova I, Karimi R, Penka E F, Brichta J P, Lassonde P, Fu X, Kieffer J C, Bandrauk A D, Litvinyuk I, Sanderson J and Légaré F 2011 *Phys. Rev. Lett.* **107** 063201
[42] Alnaser A S, Voss S, Tong X M, Maharjan C M, Ranitovic P, Ulrich B, Osipov T, Shan B, Chang Z and Cocke C L 2004 *Phys. Rev. Lett.* **93** 113003